

1 **Variable freshwater influences on the abundance of *Vibrio vulnificus* in a**  
2 **tropical urban estuary**

3

4 Olivia D. Nigro<sup>1</sup>, La'Toya I. James-Davis<sup>2,3†</sup>, Eric Heinen De Carlo<sup>3</sup>, Yuan-Hui Li<sup>3</sup>, Grieg  
5 F. Steward<sup>2,3\*</sup>

6

7 <sup>1</sup>Department of Natural Science, Hawai'i Pacific University, Honolulu, HI

8 <sup>2</sup>Daniel K. Inouye Center for Microbial Oceanography—Research and Education,  
9 School of Ocean and Earth Science and Technology (SOEST), University of Hawai'i at  
10 Mānoa, Honolulu, Hawai'i

11 <sup>3</sup>Department of Oceanography, School of Ocean and Earth Science and Technology  
12 (SOEST), University of Hawai'i at Mānoa, Honolulu, Hawai'i

13

14 †Present address: 3551 Roger Brooke Drive, JBSA Ft. Sam Houston, San Antonio, TX  
15 78234

16

17 \* Contact: Phone 808-354-1652; email [grieg@hawaii.edu](mailto:grieg@hawaii.edu)

18

19

## 20 ABSTRACT

21 To better understand the controls on the opportunistic human pathogen  
22 *Vibrio vulnificus* in warm tropical waters, we conducted a year-long investigation in  
23 the Ala Wai Canal, a channelized estuary in Honolulu, HI. The abundance of *V.*  
24 *vulnificus* as determined by qPCR of the hemolysin gene (*vvhA*), varied spatially and  
25 temporally over four orders of magnitude ( $\leq 3$  to  $14,000 \text{ mL}^{-1}$ ). Unlike in temperate  
26 and subtropical systems, temperatures were persistently warm ( $19\text{--}31^\circ\text{C}$ ) and  
27 explained little of the variability in *V. vulnificus* abundance. Salinity (1–36 ppt) had a  
28 significant, but non-linear, relationship with *V. vulnificus* abundance with highest  
29 abundances ( $> 2,500 \text{ mL}^{-1}$ ) observed only at salinities from 7 to 22 ppt. *V. vulnificus*  
30 abundances were lower on average in the summer dry season when waters were  
31 warmer but more saline. Highest canal-wide average abundances were observed  
32 during a time of modest rainfall when moderate salinities and elevated  
33 concentrations of reduced nitrogen species and silica suggested a groundwater  
34 influence. Distinguishing the abundances of two genotypes of *V. vulnificus* (C-type  
35 and E-type) suggest that C-type strains, which are responsible for most human  
36 infections, were usually less abundant (25% on average), but their relative  
37 contribution was greater at higher salinities, suggesting a broader salinity tolerance.  
38 Generalized regression models suggested up to 67% of sample-to-sample variation  
39 in log-transformed *V. vulnificus* abundance was explained ( $n = 202$ ) using the  
40 measured environmental variables, and up to 97% of the monthly variation in canal-  
41 wide average concentrations ( $n = 13$ ) was explained with the best subset of four  
42 variables.

## 43 IMPORTANCE

44 Our data illustrate that, in the absence of strong seasonal variation in water  
45 temperature in the tropics, variation in salinity driven by rainfall becomes a primary  
46 controlling variable on *V. vulnificus* abundance. There is thus a tendency for a  
47 rainfall-driven seasonal cycle in *V. vulnificus* abundance that is inverted from the

48 temperature-driven seasonal cycle at higher latitudes. However, stochasticity in  
49 rainfall and its non-linear, indirect effects on *V. vulnificus* concentration means that  
50 high abundances can occur at any location in the canal at any time of year, making it  
51 challenging to predict concentrations of this pathogen at high temporal or spatial  
52 resolution. Much of the variability in canal-wide average concentrations, on the  
53 other hand, was explained by a few variables that reflect the magnitude of  
54 freshwater input to the system, suggesting that relative risk of exposure to this  
55 pathogen could be predicted for the system as a whole. [at 148 out of 150 words  
56 max]

## 57 **INTRODUCTION**

58 The bacterium *V. vulnificus* is an opportunistic and formidable human  
59 pathogen that has a world-wide distribution, in a variety of marine and estuarine  
60 environments (1). In humans, *V. vulnificus* may cause a range of illnesses that  
61 includes gastroenteritis, necrotizing fasciitis and septicemia (2). Infections occur as  
62 a result of ingestion of contaminated seafood (3) or via wound exposure to waters  
63 (4). Strains vary in their propensity to cause disease in humans, with certain  
64 genotypically distinguishable strains much more commonly, but not exclusively,  
65 associated with disease in humans (5). The exact mechanisms of virulence in *V.*  
66 *vulnificus*, and the genes responsible for the onset of illness, have yet to be  
67 determined, but a number of correlative biomarkers have been used to discriminate  
68 those strains most commonly associated with human disease (6). Variations in the  
69 16S rRNA gene, for example, have been used in PCR assays to discriminate “A-type”  
70 strains from “B-type” strains (7, 8), the latter of which predominate among clinical  
71 isolates. Another commonly used marker is the 200 bp segment of the virulence-  
72 correlated gene that resolves the gene variants *vcgC* or “C-type” strains from *vcgE* or  
73 “E-type” strains (9). PCR-based analysis of fifty-five *V. vulnificus* isolates indicated  
74 that 90% of the strains isolated from infected patients were of the C-type (clinical),  
75 while 93% of the strains isolated from the environmental samples were E-type  
76 (environmental). Subsequent analyses revealed broader genomic differences along

77 with physiological differences between these lineages suggesting that they are  
78 distinct ecotypes that may be better adapted for either environmental growth (E-  
79 type) vs. stress tolerance (C-type) (10). These biomarkers are largely congruent,  
80 with the common environmental strains being A-type/E-type, and the majority of  
81 clinical isolates being B-type/C-type, although all types can cause disease in humans  
82 (11).

83 Studies of *V. vulnificus* in temperate and subtropical waters have shown that  
84 warmer temperatures increase the frequency of detection (12–15). Quantification  
85 over an annual cycle reveals a clear temperature-driven seasonal signal, with the  
86 highest concentrations of *V. vulnificus* occurring in warm summer months (16–19)  
87 and culturable cells declining dramatically at temperatures below 13 °C (6). *V.*  
88 *vulnificus* abundance is also influenced by salinity (19–21), thriving in conditions of  
89 both warm temperatures and moderate salinities (5). The environmental patterns of  
90 abundance are consistent with observations of *V. vulnificus* growth under controlled  
91 laboratory conditions (12, 22) that show increasing growth rates up to around 37  
92 °C, and a broad salinity tolerance with fastest growth rates between 5–25 ppt.  
93 Correlation models of environmental data support the idea that temperature and  
94 salinity are two of the most important variables controlling *V. vulnificus* abundance,  
95 but their relative importance depends on the ranges over which they are sampled .  
96 (21, 23–26).

97 In temperate environments, the incidence of *V. vulnificus* infection tracks the  
98 seasonal environmental abundances of the pathogen, with the most infections  
99 occurring during the warm summer months (6). It follows that the inhabitants of  
100 sub-tropical, and especially tropical areas, where air and water temperatures are  
101 warm year-round, would be particularly vulnerable to *V. vulnificus* infection. Indeed,  
102 according to available surveillance data for the years 2003–2008 (27–29), Hawai'i  
103 had the fifth highest incidence of non-food-borne *V. vulnificus* infections in the U.S.,  
104 trailing only four gulf states (Florida, Louisiana, Mississippi, and Texas). On a per  
105 capita basis, it was the highest in the nation. Despite higher incidence of *V. vulnificus*  
106 wound infections, primarily from recreational waters, there has been little data  
107 collected on *Vibrio vulnificus* in the coastal waters of Hawai'i (30, 31) and scant data

108 on the ecology of *V. vulnificus* in tropical waters in general (20). Consequently, we  
109 initiated an investigation of the abundance and dynamics of *V. vulnificus* in the Ala  
110 Wai Canal and Harbor.

111 The Ala Wai canal provides partially channelized drainage for two  
112 watersheds. Although it is not designated as a recreational waterway, the canal is  
113 used extensively for boating and fishing. Flow down the canal varies as a function of  
114 tide and of rainfall, the latter driving surface runoff (streams and storm drains) and,  
115 with some hysteresis, groundwater seepage. Salinity varies widely in the canal, as a  
116 function of depth, overall stream flow, position in the canal relative to the  
117 freshwater sources, and tidal forcing. Water temperature, on the other hand, varies  
118 over a relatively narrow range compared to temperate systems. Because of the  
119 seasonality in rainfall in Hawaii, with higher precipitation in winter months (32), we  
120 hypothesized that there could be an inverse seasonal pattern in *V. vulnificus*  
121 abundance driven by salinity compared to the strongly temperature-driven patterns  
122 in temperate waters.

123 Our objectives with this study were to document the temporal spatial  
124 variability of *V. vulnificus* total abundance and strain composition (C-type vs. E-  
125 Type) in the estuarine waters of the Ala Wai Canal and Harbor and to determine  
126 how abundance was related to environmental variables. The goal was to better  
127 understand the environmental controls on *V. vulnificus* in tropical estuarine waters  
128 and to assess the prospects for modeling pathogen abundance.

## 129 **MATERIALS AND METHODS**

### 130 **Study Site**

131 Sampling took place in the Ala Wai Canal (Fig. 1), a 3.1 km long, engineered  
132 waterway located on the southern coast of O'ahu that separates Waikiki and urban  
133 Honolulu (33). A watershed that covers 42.4 km<sup>2</sup> drains into the Ala Wai Canal via  
134 the Mānoa and Palolo Streams, which merge to form the Mānoa-Palolo Stream prior  
135 to entering the canal, and the Makiki Stream, all of which run through urban areas

136 before reaching the canal. As a consequence, the streams are contaminated with a  
137 variety of anthropogenic substances and their convergence in the Ala Wai Canal has  
138 contributed to its pollution and eutrophication (34, 35). The influx of fresh water  
139 from the streams creates a salinity gradient with a typical salt-wedge structure.  
140 Tidal flow causes seawater to flow landward on the flood tide and seaward on the  
141 ebb tide and remain at depth. The freshwater streams flow seaward on all tides  
142 creating a freshened water surface layer estimated to extend to 0.5 m depth on  
143 average, but which is highly variable both in salinity and thickness (36). Sediments  
144 are continually deposited in the canal at the mouth of the Mānoa-Palolo Stream  
145 causing the build-up of a sill that restricts flushing of deep water in the uppermost  
146 section of the canal.

#### 147 **Sampling locations, dates, and times**

148         Sampling of the Ala Wai Canal spanned 13 months beginning March 17, 2008  
149 and concluding on March 10, 2009, covering the nominal dry summer (April–  
150 September) and rainy winter (October–March) months. Samples were collected  
151 monthly at twelve sites in the Ala Wai Canal numbered (1 and 5–15) by distance  
152 from the shallow, upper section of the canal (Site 1) to the Ala Wai Harbor (Site 15).  
153 Site 9 was just inside the mouth of Mānoa-Palolo Stream and Site 12 was at the  
154 mouth of Makiki Stream (Fig. 1, Supplemental Table S1). Missing site numbers 2–4  
155 referred to other samplings at Site 1 that were not used in this study. Sampling at a  
156 higher temporal resolution was also conducted in the dry and rainy seasons to  
157 assess changes on shorter time scales. Samples were collected weekly at all sites for  
158 four weeks from June 26–July 17, 2008 and again for three weeks from February  
159 22–March 10, 2009. Samples were also collected at a reduced number of sites (Sites  
160 5, 9, 12, 14) daily for six days from July 10–15, 2008 and daily for five days from  
161 March 2–6, 2009, and once every three hours (trihoral) for twenty-four hours at  
162 Sites 5, 9, and 14 from July 15 to July 16, 2008.

## 163 **Rainfall and streamflow**

164           Rainfall data collected by National Weather Service rain gauges (part of the  
165 Hawai'i Hydronet System) at 15-minute intervals were retrieved from the online  
166 resource (<https://www.weather.gov/hfo/hydronet-data>). Data from two gauges  
167 were selected for analysis. The first was HI-18 (NOAA# MNLH1), which is located  
168 near the origin of Mānoa Stream (N21.3161 W157.8142) at an elevation of 150 m in  
169 Manoa Valley ("Valley" rainfall). The second is HI-26 (ALOH1), which is located at  
170 Aloha Tower (N21.3060 W157.8662) in downtown Honolulu near sea level (15 m)  
171 at the coast ("Coastal" rainfall). From these data, average daily rainfall for all  
172 sampling months was determined, as well as total rainfall from each 24-hour period  
173 prior to sampling. Data on tidal flux were obtained from the National Ocean Service  
174 (NOS), using tide gauge number 1612340. Stream flow data were obtained from the  
175 United States Geological survey ([waterdata.usgs.gov/usa/nwis/uv?16247100](http://waterdata.usgs.gov/usa/nwis/uv?16247100)) for  
176 the Mānoa-Palolo Stream gauge #16247100.

## 177 **Water sample collection and processing**

178           Whole water samples were collected from the top 10–30 cm at all sites in  
179 acid-washed bottles with a pole sampler and stored on ice (except for samples used  
180 for culturing, which were kept at ~15 °C with cold packs) and transported to the  
181 laboratory within three hours of collection. Subsamples (ca. 25 mL) for nutrient  
182 analysis (n = 207–211) were frozen and shipped on dry ice to the Oregon State  
183 University nutrient analysis facility for determination of dissolved silica, phosphate,  
184 nitrate plus nitrite, nitrite, and ammonium concentrations (37). Nutrient  
185 concentrations were measured during every sampling event excluding two weekly  
186 sampling events in July 2008 (July 3 and 7). The values for the mean, number of  
187 samples, median, minimum and maximum of the measured nutrients have been  
188 previously reported (38).

189           For particulate carbon (PC) or nitrogen (PN) and chlorophyll a (chl a)  
190 measurements, subsamples (25–200 ml) were filtered onto pre-combusted glass-  
191 fiber filters (GF/F, Whatman) in duplicate and stored frozen until analysis. For PC

192 and PN (n = 199), filters were pelletized and combusted in a high-temperature  
193 combustion CN analyzer, the CE-440 CHN elemental analyzer (Exeter Analytical)  
194 following HOT program protocols (39). Filters for chl a analysis (n = 194) were  
195 extracted in 100% acetone at -20°C for 7 days. Fluorescence of extracts and  
196 standards were measured using a Turner AU10 fluorometer before and after  
197 acidification (40).

198 Samples for bacteria counts (n = 219) were fixed with filtered (0.2 µm)  
199 formaldehyde (10% w/v final concentration) in a cryovial (Nalgene) and stored at -  
200 80 °C. Total bacteria were counted by thawing samples, staining with SYBR Green I,  
201 and analyzing on an acoustic focusing flow cytometer (Attune; Thermo Fisher  
202 Scientific).

203 Samples for molecular analysis (100– 550 mL) were pressure filtered via  
204 peristaltic pump through 0.22 µm polyethersulfone filter capsule (Sterivex,  
205 Millipore), then stored at -80 °C until extracted.

## 206 **Cultivation on vibrio selective medium**

207 For five of the monthly samplings (Mar, Jun, Sep, Dec 2008, and Mar 2009),  
208 water samples were filtered through 0.45 µm pore size, mixed cellulose ester filters  
209 (47 mm, GN-6; Pall) and filters were placed face-up on the vibrio-selective medium  
210 CHROMagar Vibrio (DRG Intl.). After overnight incubation, blue colonies were  
211 enumerated as putative *V. vulnificus*.

## 212 **DNA extraction and purification**

213 DNA was extracted from the Sterivex filters using the Masterpure™ Nucleic  
214 Acid Extraction Kit (Epicentre). Six-hundred microliters of Masterpure™ Tissue and  
215 Cell Lysis Solution containing recommended quantities of proteinase K were added  
216 to each Sterivex filter. The ends of the filters were sealed and the filters incubated  
217 on a rotisserie in a hybridization oven at 65 °C for 15 minutes. Fluid was recovered  
218 from filter housing by aspiration with a syringe. The filling with buffer, incubation,  
219 and buffer recovery steps were repeated twice more and the combined extract from  
220 all three rounds was pooled (total volume ca. 1.8 ml). Three-hundred microliters of



221 the pooled extract was processed according to the Masterpure™ Kit guidelines and  
222 the remainder was archived. Accounting for all of the raw extract volume, total DNA  
223 yields ranged from 1–540  $\mu\text{g L}^{-1}$  of canal water (geometric mean of 30  $\mu\text{g L}^{-1}$ ).  
224 Following initial purification, the resuspended DNA (200  $\mu\text{L}$ ) was passed through a  
225 spin column containing acid-washed polyvinylpolypyrrolidone (PVPP) in an effort  
226 to remove any residual inhibitors (41). DNA concentration in each sample was  
227 quantified fluorometrically (Quant-iT Broad Range DNA kit, Life Technologies) both  
228 before and after the PVPP purification step to account for losses incurred during the  
229 purification stage (average recovery 60%). Geometric mean concentration of DNA in  
230 the final purified extracts was 7  $\text{ng } \mu\text{L}^{-1}$  (range 0.1–54  $\text{ng } \mu\text{L}^{-1}$ ).

### 231 **Quantitative PCR**

232 Total *V. vulnificus* was estimated by TaqMan qPCR targeting the hemolysin  
233 gene (*vvhA*) using primer and probe sequences reported by Campbell and Wright  
234 (42). Quantification of C-type *V. vulnificus* used the primers and probes targeting the  
235 virulence-correlated gene variant (*vcgC*) from Baker-Austin et al. (43). E-type *V.*  
236 *vulnificus* was calculated as the difference in concentration between the two assays.  
237 Both assays were prepared as 25- $\mu\text{L}$  reactions with 12.5  $\mu\text{L}$  of TaqMan Universal  
238 PCR Master Mix (Applied Biosystems), 1.5  $\mu\text{g } \mu\text{L}^{-1}$  final concentration of non-  
239 acetylated bovine serum albumin (Applied Biosystems) and 0.25–0.9  $\mu\text{M}$  each of the  
240 appropriate primers and probe (Supplemental Table S2), 2–5  $\mu\text{L}$  of DNA template,  
241 and water as needed. For *vvhA* assay, primers were added at 0.9  $\mu\text{M}$  each and the  
242 probe at 0.25  $\mu\text{M}$ . For the *vcgC* assay, primers and probe were each added at 0.5  $\mu\text{M}$   
243 final concentrations. Cycling conditions consisted of initial denaturation at 95 °C (10  
244 min), then 40 cycles of 95 °C (15 s) and 60 °C (60 s). All qPCR reactions were  
245 performed in triplicate with DNA template in the final replicate diluted 10-fold (up  
246 to 50-fold) to check for inhibition (44) and with additional replication as needed to  
247 repeat inhibited samples at the higher dilutions. The cycling protocol consisted of an  
248 initial denaturation at 95 °C for 10 minutes, followed by 40 cycles of 95 °C for 15 s  
249 and 60 °C for 60–90 s. The amplified PCR product was detected by monitoring the  
250 increase in fluorescence signal generated from the 6-carboxyfluorescein-labeled

251 probe using a Realplex<sup>2</sup> Mastercycler (Eppendorf). Data were analyzed using  
252 realplex software (Eppendorf) to determine cycle threshold ( $C_t$ ) values. A standard  
253 curve of serial 10-fold dilutions of genomic DNA (*V. vulnificus* strain YJ016) was run  
254 in triplicate along with the samples.

## 255 **Statistical treatment of data**

256 Statistical analyses were conducted using JMP Pro 15 (SAS Institute, Inc.).  
257 Concentrations of *V. vulnificus* (CFU or *vvhA* gene copies mL<sup>-1</sup>), total bacteria, chl *a*,  
258 nutrients, PC, and PN were log transformed and rainfall and streamflow were cube-  
259 root transformed in order to normalize the data for multivariate analyses. For some  
260 analyses, sites were clustered into categories of “Upper canal” (Sites 1, 5–8) and  
261 “Lower canal” (Sites 10, 11, 13–15) based on whether they were landward or  
262 seaward of the sediment sill deposited at the mouth of the Mānoa-Palolo Stream.  
263 Comparison of means between two samples were conducted with t-tests assuming  
264 unequal variance or by the non-parametric Komlgorov-Smirnov Asymptotic Test for  
265 data that could not be readily normalized by transformation. Comparisons of means  
266 among three or more samples were conducted by ANOVA with a post-hoc Tukey-  
267 Kramer test of honestly significant difference. Factor analysis was conducted on  
268 *vvhA* and nutrient data using principal components with varimax rotation. For  
269 multiple linear regression, the data were split into two subsets (salinity < 12 or ≥12  
270 ppt), because of the non-linearity in the relationship between *V. vulnificus* and  
271 salinity (21). Multiple linear regression models were also conducted on data  
272 covering the entire salinity range by either including a quadratic term for salinity  
273 (24, 45) or a derived variable  $\Delta\text{Sal}_{\text{opt}}$ , which is the absolute value of difference  
274 between the sample salinity and an optimum salinity set as 12 ppt (46). Variables  
275 for constructing generalized regression models on each subset were selected using  
276 the Akaike Information Criterion by screening for the subsets that produced the best  
277 fit among all possible models. Among equivalent subsets in the “green zone” (AICc to  
278 AICc+4), either the subset with the best fit or with the fewest variables was selected  
279 as noted in the text.

280 Out of 243 total qPCR assays for *V. vulnificus* abundance, seventeen (ca. 7%)  
281 had issues that made them unreliable or unavailable (inhibition, below the reporting  
282 limit for the assay, or absence of data). In thirteen of these instances, abundances  
283 were instead inferred from blue colony counts on CHROMagar Vibrio medium  
284 (Supplemental Methods), based on the strong correlation ( $r = 0.8$ ) between log-  
285 transformed concentrations of blue colony counts and *vvhA* gene copy numbers  
286 (Supplemental Fig. S1).

## 287 RESULTS

### 288 Variability of the habitat

289 Rainfall in Mānoa Valley, one of the major watersheds draining into the canal,  
290 varied from 0 to 15.8 cm in the 24-hour period preceding each sampling event. The  
291 average rainfall prior to samplings in the rainy season (Oct–Mar) was 3.7 cm, which  
292 was significantly higher ( $p = 0.0054$ ) by an order of magnitude compared to the  
293 average in the dry season (Apr–Sep) of 0.27 cm (Supplemental Figure S2). Flow  
294 from the Mānoa-Palolo Stream varied from 0.4 to 2.6  $\text{m}^3 \text{s}^{-1}$  on sampling days and  
295 was strongly correlated with the prior 24-hr rainfall in Mānoa Valley ( $r = 0.87$ ,  $n =$   
296 13,  $p < 0.0001$ ; Supplemental Table S3). Both the canal-wide average salinity and  
297 temperature for the monthly samplings ( $n = 13$ ) had significant negative  
298 correlations with prior 24-hr rainfall ( $r = -0.84$ ,  $p = 0.0003$  and  $r = -0.86$ ,  $p = 0.0002$ ,  
299 respectively).

300 Over the course of the 13-month study, measured surface water salinities in  
301 the Ala Wai Canal varied from 1 to 36 ppt (mean of 24 ppt) and temperatures from  
302 19.2 to 31.8 °C (mean of 27 °C; Table 1). Salinity was highly variable throughout the  
303 study area reaching maxima of  $\geq 29$  ppt at every site and minima of  $\leq 5$  ppt at least  
304 once at each site except Site 15, which is the most seaward site in the harbor  
305 (minimum salinity of 11 ppt). As a consequence, there was no significant difference  
306 in average salinity among sites (ANOVA,  $p > 0.07$ ). When samples were clustered by  
307 general location, average salinity in the upper and lower canal were not significantly

308 different ( $p = .7818$ ), but the combined stream mouth sites had significantly lower  
309 salinity on average than either the upper ( $p = .0083$ ) or lower ( $p = .0016$ ) canal sites.

310 All of the measured variables (Table 1) except silica and nitrite displayed  
311 overall significant positive or negative significant correlations with salinity  
312 (Supplemental Table S4), but the correlation coefficients were low in many cases  
313 because of non-linearity in the relationships (Fig. 2). Temperature displayed a  
314 significant, linear positive correlation with salinity ( $r = 0.65$ ,  $n = 242$ ,  $p < .0001$ ).  
315 Correlation and regression analyses for all other variables vs. salinity are reported  
316 for log transformed data. Concentrations of chl *a* (range 0.4–512  $\mu\text{g L}^{-1}$ ) showed a  
317 significant positive, linear (Fig. 2a) correlation with salinity ( $r = 0.49$ ,  $n = 194$ ,  $p <$   
318  $0.0001$ ). Concentrations of total bacteria (range  $0.47 \times 10^6$  to  $11 \times 10^6$   $\text{mL}^{-1}$ ) also  
319 showed a significant positive correlation with salinity ( $r = 0.29$ ,  $n = 219$ ;  $p < 0.0001$ ),  
320 but the relationship was non-linear (Fig. 2c). Particulate carbon (range 15–5,600  
321  $\mu\text{M}$ ) had a non-linear relationship with salinity (Fig. 2d) that resulted in an overall  
322 weak but significant negative correlation ( $r = -0.25$ ,  $n = 199$ ,  $p = 0.0003$ ).

323 Of the dissolved inorganic nutrients, only phosphate (range 0.2–8.7  $\mu\text{M}$ ) had  
324 a linear relationship with salinity (Fig. 2e) and displayed a significant negative  
325 correlation ( $r = -0.46$ ,  $n = 211$ ,  $p < 0.0001$ ). Concentrations of silica (11–490  $\mu\text{M}$ ),  
326 nitrate (0.02–260  $\mu\text{M}$ ), nitrite (0.04–3.3  $\mu\text{M}$ ), and ammonia (0.94–22  $\mu\text{M}$ ) all  
327 displayed significant, non-linear relationships with salinity (Fig. 2f-i), with highest  
328 values occurring at moderate salinities. Despite the non-linear relationships, there  
329 were significant negative correlations between salinity and either nitrate ( $r = -0.32$ ,  
330  $p < 0.0001$ ) or ammonia ( $r = -0.44$ ,  $p < 0.0001$ ). Silica and nitrite, on the other hand,  
331 showed highly significant, non-linear relationships with salinity (Fig. 2f, h), that  
332 resulted in low and insignificant correlation coefficients.

333 When sites were clustered by location, most nutrients (nitrate, ammonia,  
334 phosphate, silica, but not nitrite), particulate carbon, chl *a*, and total bacteria were  
335 all significantly higher ( $p < 0.01$ ) in the upper canal sites than the lower canal sites.

### 336 **Temporal and spatial variability of *V. vulnificus***

337 Concentrations of the *vvhA* gene (a proxy for *V. vulnificus* abundance) varied  
338 over four orders of magnitude in space and over time (Fig. 3) from 3 to 13,700 mL<sup>-1</sup>  
339 with overall geometric mean concentration for all samplings of 68 mL<sup>-1</sup> (n = 239;  
340 Table 1). Concentrations of *vvhA* at any given site were highly variable over time  
341 with values that were above average or below average occurring at some point at  
342 every location. Although spatial and temporal variability were low during the  
343 trihoral sampling over the course of one day in July, larger variations were seen on  
344 daily or longer time scales. The most dramatic variation is the change from above  
345 average to below average concentrations at every site in the span of 15 days  
346 (October 27 to November 11, 2008).

347 Despite the high variability, average log-transformed *vvhA* concentrations in  
348 the rainy season ( $1.98 \pm 0.72$ ) were significantly higher (unpaired t-test,  $p = .0013$ )  
349 than the dry season ( $1.72 \pm 0.50$ ; Supplemental Fig. S2). None of the individual  
350 sites had an annual average *vvhA* concentration that was significantly different from  
351 any of the others (ANOVA, post-hoc Tukey,  $p \geq .63$ ). However, excluding the stream  
352 mouth sites, the annual average concentration of log-transformed *vvhA* for the five  
353 sites in the upper canal ( $2.04 \pm 0.74$ ) was significantly higher (n = 65 at each site;  
354 unpaired t-test,  $p = .0110$ ) than the annual average for five sites in the lower canal  
355 ( $1.75 \pm 0.70$ ).

### 356 **Relationship of *V. vulnificus* to temperature and salinity**

357 Log-transformed concentrations of *vvhA* displayed a weak, but significant,  
358 negative correlation ( $r = -0.174$ ,  $p = .0071$ ) with temperature (Fig 4a). However,  
359 partial correlation analysis indicates that the relationship between log[*vvhA*] and  
360 temperature is weakly positive, but significant ( $r = 0.258$ ,  $p < .0001$ ) when  
361 accounting for the effect of salinity and other variables. The relationship of  
362 log[*vvhA*] with salinity was non-linear with a peak around 12 ppt (Fig. 4b). Linear  
363 regression analysis with samples with salinity < 12 or  $\geq 12$  ppt showed that *vvhA*  
364 increased significantly ( $r^2 = 0.315$ ; F test,  $p = .0001$ ) as a function of salinity over the

365 lower range and decreased significantly ( $r^2 = 0.492$ ; F test  $p < .0001$ ) over the  
366 higher range.

367 Concentrations of clinical, or C-type, *V. vulnificus* were usually lower than  
368 those of environmental, or E-type, and accounted for 26% of the total *V. vulnificus* on  
369 average across all samplings for which data were available ( $n = 219$ ), indicating that  
370 communities were most often dominated by E-type. Both C-type and E-type *V.*  
371 *vulnificus* were most abundant at moderate salinities and declined as a function of  
372 salinity, but C-type declined at a lower rate. As a consequence, the contribution of C-  
373 type tended to increase as a function of salinity. Samples in which C-type accounted  
374 for >50% of the total ( $n = 39$ ) were only observed in higher salinity waters (Fig. 4b)  
375 and the % C-type was significantly higher (Kolmogorov-Smirnov;  $p = 0.0164$ ) in  
376 higher salinity samples ( $\geq 25$  ppt,  $n = 146$ ) than samples having lower salinity ( $< 25$   
377 ppt,  $n = 73$ ; Supplemental Fig. S3).

### 378 **Relationship between *V. vulnificus* and additional variables**

379 To understand additional factors that may be important in controlling *V.*  
380 *vulnificus* in this habitat, factor analysis was conducted with *vvhA*, temperature,  
381 salinity, and nutrient data (Fig. 5a). Two factors had eigenvalues  $> 1$ . The strongest  
382 positive correlations ( $r \geq 0.4$ ) were between *vvhA* and silica or reduced nitrogen  
383 species, which were associated with Factor 1, and strong negative correlations ( $r \leq -$   
384  $0.4$ ) were found between salinity and *vvhA*, ammonia, and phosphate along Factor 2.  
385 Plots of the factor loading values with points coded by rainfall and streamflow (Fig  
386 5b) illustrate the relationship between these two related indicators of freshwater  
387 input and salinity along the Factor 2 axis. Coding the points by log *vvhA*  
388 concentration and silica concentration illustrates the association of these variables  
389 (along with reduced nitrogen species) with Factor 1. Overall the highest  
390 concentrations of *vvhA* occurred at moderate rainfall in the valley, but relatively low  
391 streamflow, and elevated concentrations of silica.

392 Generalized regression models for predicting *vvhA* concentrations over the  
393 two different salinity ranges were constructed using the overall best subset ( $< 12$   
394 ppt model) or the best subset having the minimum number of variables ( $\geq 12$  ppt

395 model). Only properties intrinsic to the individual samples were included in this  
396 analysis (i.e., tides, rainfall and streamflow were not considered). For samples with  
397 salinities < 12 ppt (n = 39 out of 41 samples, because of missing nutrient data) a  
398 subset of four (temperature, nitrite, silica, and PC) out of eight variables explained  
399 75% of the observed variation with the equation:

400

$$401 \quad \log[vvhA] = 0.154 \cdot T + 1.015 \cdot \log[nitrite] - 0.600 \cdot \log[silica] - 0.850 \cdot \log[PC] + 2.170$$

402

403 where  $T$  is temperature in °C, and nitrite, silica, and particulate carbon (PC) are in  
404 units of  $\mu\text{M}$  (model fit illustrated in Supplemental Fig S4a). For samples with  
405 salinities the  $\geq 12$  (n = 163 out of 198 possible samples because of missing nutrient  
406 data) a subset of just three (temperature, salinity and phosphate) out of seven  
407 variables explained 55% of the variability:

408

$$409 \quad \log[vvhA] = 0.0360 \cdot T - 0.0727 \cdot S + 0.515 \cdot \log[phosphate] + 2.835$$

410 where  $T$  is temperature in °C,  $S$  is salinity is in units of ppt, and phosphate is in units  
411 of  $\mu\text{M}$  (model fit illustrated in Supplemental Fig. S4b). PC was removed prior to  
412 variable selection in the latter model, because initial analysis showed it offered no  
413 significant explanatory power at salinities >12 ppt, and missing data would have  
414 further restricted the samples included in the analysis. When predictions from the  
415 two models were combined, 66% of the variability in  $\log(vvhA)$  over the entire  
416 salinity range was explained overall (Fig. 6).

417 Models in which either a quadratic term for salinity or the derived variable  
418  $\Delta\text{Sal}_{\text{opt}}$  were included explained similar amounts of variability ( $r^2 = 0.61$  and  $0.63$ ,  
419 respectively;  $p \leq .0001$ ) using different sets of five variables (Supplemental Fig. S5),  
420 but were slightly outperformed by the combined models above.

## 421 **System-wide controls on *V. vulnificus***

422 To smooth out inter-station variability and focus on temporal variations in  
423  $vvhA$ , canal-wide averages for the variables for each monthly sampling were also

424 analyzed in relation to system-wide drivers of rainfall and streamflow (Fig. 7). In  
425 general, average rainfall, streamflow, phosphate, silica, and *vvhA* are all below  
426 average, and salinity above average, during most of the dry season with minimal  
427 variability. During the rainy season, periodic heavy rainfall resulted in high  
428 variability with excursions in all variables well above and below their overall  
429 averages.

430 Three freshening events are evident from dips in the average salinity in the  
431 canal during the rainy season (Fig. 7). The first begins in September and peaks in  
432 October 2008 following increases in rainfall and streamflow. The average monthly  
433 rainfall increased from  $\leq 0.75$  cm d<sup>-1</sup> in the preceding months to 1.0 cm d<sup>-1</sup> in Sep-  
434 Oct, and the 24-hour antecedent rainfall for the October sampling was 2 cm (up  
435 from  $\leq 0.5$  cm in other samplings). Streamflow increased from 0.4 cm<sup>3</sup> s<sup>-1</sup> in July-  
436 August to 0.7–0.8 cm<sup>3</sup> s<sup>-1</sup> in Sep–Oct. Despite these relatively modest increases,  
437 canal-wide average salinity dropped to 8 ppt and the average silica concentrations  
438 in Sep–Oct reached their highest concentrations (223–244  $\mu$ M). Phosphate  
439 displayed only a small local peak in average concentration (2  $\mu$ M). Canal-wide  
440 average concentrations of *vvhA* reached a maximum during this event from 350  
441 (range 67–3,500 gene copies mL<sup>-1</sup> in September to an average of 2,700 (range 170 to  
442 13,700) gene copies mL<sup>-1</sup> in October. The average concentration in October was  
443 significantly higher than at any other monthly sampling (ANOVA, post-hoc Tukey,  $p$   
444  $\leq .0005$ ). At the subsequent sampling 15 days later (November), rainfall had  
445 stopped, streamflow, phosphate and silica had declined, average salinity had  
446 increased to 29 ppt and *vvhA* was at the lowest average concentration of the study  
447 with an average of 20 (range 7–63) gene copies mL<sup>-1</sup> across all sites.

448 A second, more pronounced drop in salinity occurred in December 2008 in  
449 response to heavy rainfall recorded at both the coastal and Mānoa valley rain  
450 gauges, resulting in the highest recorded streamflow (2.6 m<sup>3</sup> s<sup>-1</sup>), minima in salinity  
451 (3 ppt) and silica (34  $\mu$ M), and the highest average phosphate concentration (2.9  
452  $\mu$ M). In contrast to the previous freshening event, *vvhA* was not significantly  
453 elevated (61 gene copies mL<sup>-1</sup>) and was near the overall study average.



454 A third freshening event occurred at the time of the last sampling in March  
455 2009 as a result of heavy rainfall in Mānoa Valley, but not at the coast. Streamflow  
456 ( $1.3 \text{ m}^3 \text{ s}^{-1}$ ) was above average and intermediate between the first and second  
457 events, and salinity was again significantly reduced (4 ppt). The effects on  
458 phosphate ( $1.3 \text{ } \mu\text{M}$ ) and silica ( $87 \text{ } \mu\text{M}$ ) were modest, with phosphate being just  
459 above the long-term average and silica just below. The mean concentration of *vvhA*  
460 reached its third highest level at this time reaching 175 (range 22–811) gene copies  
461  $\text{mL}^{-1}$  after steadily increasing each month from the lowest value in November.

462 Multiple linear regression was used to determine which subset of variables  
463 best predicted canal-wide average  $\log(\text{vvhA})$  concentrations. The model resulting  
464 from the best subset out of all combinations of twelve possible variables was:

465  
466 
$$\text{Log}[\text{vvhA}]_{\text{avg}} = -1.125 \cdot \text{Streamflow} - 0.07633 \cdot \text{Salinity} + 0.00502 \cdot \text{Silica} + 0.00151 \cdot \text{PC} + 3.522$$

467  
468 where streamflow is in units of  $\text{m}^3 \text{ s}^{-1}$ , and salinity, silica, and particulate carbon  
469 (PC) are in units of  $\mu\text{M}$ . All variables are the geometric means for all sites in the  
470 canal for each monthly sampling ( $n = 13$ ). Linear regression of the observed vs.  
471 predicted *vvhA* suggests that 97% of the canal-wide average variation in *vvhA* could  
472 be explained with the selected variables (Fig. 8a).

473 A second simpler model using a minimum of readily measurable variables  
474 (salinity and rainfall) was also constructed:

475  
476 
$$\text{Log}[\text{vvhA}]_{\text{avg}} = -0.162 \cdot \text{rainfall} - 0.0956 \cdot \text{salinity} + 4.348$$

477  
478 where rainfall is average rainfall in cm for the prior 24 hours at the Mānoa Valley  
479 gauge, and salinity is canal-wide average salinity in ppt. This simpler model  
480 explained 83% of the variability in average  $\log$ -transformed concentrations of *vvhA*  
481 (Fig. 8b).

## 482 **DISCUSSION**

### 483 **Temporal and spatial variability of *V. vulnificus***

484 *V. vulnificus*, as inferred from *vvhA* gene, was consistently detected  
485 throughout the year in the Ala Wai Canal and Harbor system, but varied  
486 dramatically over space and time. Sampling on different temporal scales showed  
487 minimal variation in *V. vulnificus* within a day, but dramatic and stochastic  
488 variations on longer time scales and among sites. This suggests that factors with  
489 regular intra-day variations (e.g. tides, or daily changes in temperature and primary  
490 productivity driven by insolation) had relatively little influence on concentrations of  
491 *V. vulnificus*. The largest absolute change in the canal-wide average *vvhA*  
492 concentrations seen over the entire study occurred in a span of 2 weeks. The  
493 observation that *V. vulnificus* concentrations were higher on average in the rainy vs.  
494 dry season, yet the lowest average concentration recorded in the study also  
495 occurred in the rainy season within weeks of the highest abundances, suggests that  
496 freshwater input, which occurs stochastically, but with an underlying strong  
497 seasonal component, is the most significant contributor to variability in *V. vulnificus*  
498 abundance in this environment.

499 The results support an earlier hypothesis (21) that in tropical and some  
500 subtropical climates, where the temperature range is narrow and persistently  
501 warm, salinity is a stronger determinant than temperature of *V. vulnificus*  
502 abundance. This is consistent with the seasonal variation in *V. vulnificus* in oysters in  
503 India, which is not related to temperature, but by summer monsoonal rains  
504 lowering salinity (47). In Hawai'i, with its rainy season in winter months, there is a  
505 tendency toward a seasonal cycle in *V. vulnificus* abundance that is inverted from the  
506 pronounced temperature-driven cycle found at higher latitudes and the monsoon-  
507 driven cycle in India.

### 508 **Variable sources and influence of freshwater inputs**

509 The two major sources of freshwater to the Ala Wai canal are surface runoff  
510 (primarily point source from streams and storm drains) and groundwater seeps.

511 Compared to surface runoff, groundwater in Hawai'i tends to be enriched in silica as  
512 a result of prolonged water-rock interactions (48) and depleted in phosphate as a  
513 result of interactions with lateritic soils containing high concentrations of iron and  
514 aluminum oxyhydroxides (48, 49). These differences, along with information on  
515 rainfall and streamflow, are helpful in identifying the primary source of the  
516 freshwater entering the canal. In the factor analysis, Factor 1 may be interpreted as  
517 a latent variable for groundwater (high loading for silica, but low for phosphate),  
518 and Factor 2 as a latent variable for (negative) surface runoff (high, but opposing,  
519 loading of salinity and phosphate). Plots of the loading scores reinforce the  
520 observation that *V. vulnificus* tended to be highest at moderate salinities and suggest  
521 that groundwater was a relatively more important source of freshwater input under  
522 those conditions (low streamflow, but elevated silica). When rainfall was highest,  
523 surface runoff contributed more to freshwater input (highest streamflows with high  
524 phosphate, low silica) and was associated with lower concentrations of *vvhA*.

525 This variable relationship between *vvhA* and freshwater source was also  
526 discernible in the temporal changes in variables when averaged across all canal  
527 sites. Of the three major freshening events, the first, with relatively high silica and  
528 low phosphate, suggests a significant contribution from groundwater. This is  
529 consistent with the observation of significant freshening, despite only modest  
530 increases in stream flow compared to the summer months. This presumed increase  
531 in groundwater input appears to have been driven by a moderate increase in  
532 monthly average rainfall in both September and October, coupled with a modest  
533 increase in average rainfall during the 24 hours preceding sampling that was  
534 greater at higher elevations in the watershed, than locally.

535 The second freshening event, with a high concentration of phosphate but low  
536 silica, appears to be dominated by surface runoff, resulted from a Kona storm on the  
537 south shore of Oahu (38). A Kona storm is a rain event that deviates from the  
538 normal northeasterly trade-wind driven patterns that govern Hawaii's weather, and  
539 occurs when southwestern Kona winds bring heavy rains to the southern shore of  
540 Oahu. This storm resulted in unusually high rainfall, both higher in the watershed  
541 and locally, in the 24 hours prior to sampling.

542           The third freshening event on March 10, 2009 appears to have a source  
543 signature that is intermediate to the two prior events in terms of stream flow and  
544 silica. This is consistent with an average rainfall in the preceding 24 hours in the  
545 watershed that was high enough to increase downstream runoff and groundwater  
546 discharge into the canal (as in the previous event), but with limited local  
547 precipitation that, unlike the previous event, did not contribute appreciably to  
548 surface runoff.

549           The concentrations of *vvhA* during these three events suggest that the  
550 magnitude, if not the sources, of the freshwater input to the canal has a large  
551 influence on *V. vulnificus* abundances. The mixing of freshwater with the seawater in  
552 the canal is expected to have competing influences on *V. vulnificus*, because it  
553 simultaneously alters temperature, salinity, and residence time. At sustained,  
554 moderate levels of freshwater input (such as that from ground water intrusion  
555 driven by moderate rainfall higher in the watershed), both the temperature drop  
556 and decrease in residence time are relatively small, but the freshening is sufficient  
557 to result in salinities that are optimal for *V. vulnificus*, thus explaining the unusually  
558 high abundance of *V. vulnificus* in September and October 2008. During unusually  
559 intense storms, especially with high rainfall lower in the watershed (December  
560 2008), the very high levels of surface runoff appear to suppress abundances of *V.*  
561 *vulnificus* in the canal. This is likely a result of the simultaneous reduction in growth  
562 rate (caused by decreases in both temperature and salinity to below optimum) and  
563 reduced residence time of water in the canal. Gonzalez {Gonzalez:1971to} observed  
564 an inverse relationship between streamflow and residence time of runoff waters in  
565 the Ala Wai Canal.

566           Although intense storms can temporarily suppress the canal-wide average  
567 concentrations of *V. vulnificus* in the canal/harbor system, the actual changes are  
568 site-specific. We observed, for example, that during the December 2008 storm, *V.*  
569 *vulnificus* abundance, despite a lower canal-wide average, was higher than average  
570 at Site 15, the most seaward site located in the Ala Wai Boat Harbor. In this location,  
571 salinity was temporarily reduced to 13 (in the optimal range for *V. vulnificus*)  
572 compared to the typical average salinity for this site of  $\geq 30$  (38). Salinity remained

573 below the average in the harbor for 16 hours following the cessation of rainfall. This  
574 suggests that the sites posing the highest risk of infection by *V. vulnificus* will vary  
575 depending on the rainfall patterns and can even include the harbor which usually  
576 had some of lowest concentrations. This condition-dependent elevated risk in the  
577 harbor is consistent with the unfortunate incident of infection and death of an  
578 individual who had open wounds exposed to harbor water following a long period  
579 of intense rainfall (50).

### 580 **Patterns of *V. vulnificus* strain abundance**

581 C-type *V. vulnificus* are the strains most frequently associated with infections  
582 in humans (9), but are often less abundant than E-type in environmental samples  
583 (9, 51). This appeared to be the case in our study site with C-type *V. vulnificus*  
584 accounting for an estimated 25% on average. The percentage was highly variable,  
585 however, and our observation that the C-type *V. vulnificus* tended to make up a  
586 higher percentage of the total at higher salinities (despite declining in absolute  
587 abundance) is consistent with some previous observations. Williams et al. (2017),  
588 for example, observed a negative influence of salinity on the abundance of E-type  
589 and C-type strains, but the effect was greater for E-type (51). Lin and Schwartz  
590 (2003) observed that when temperature decreased and salinity increased, in situ  
591 abundance of 16S rRNA A-type strains (analogous to E-type) decreased while B-type  
592 (analogous to C-type) increased and temporarily became the dominant genotype  
593 (52). Other studies in high salinity (> 32 ppt) coastal waters have found that either a  
594 majority (7) or all (53) of the isolates obtained were of B-type (C-Type). These  
595 observations support the contention that these different genotypes reflect distinct  
596 ecotypes, with the C-type having greater stress tolerance (10).

597 Multiple linear regression analysis was used to model *V. vulnificus* abundance  
598 using a reduced number of variables. Although these variables explained a  
599 significant percentage of the variability in *V. vulnificus* abundance, a great deal of  
600 sample-to-sample variability remains unexplained, which is not uncommon (21, 26).  
601 Predicting system-wide average concentrations of *V. vulnificus*, on the other hand,  
602 was much more successful. A model with the best subset of four variables explained

603 97% of the variability, and much simpler model relying on only two readily  
604 obtainable measurements (rainfall and salinity), still accounted for much of the  
605 variability and might prove more useful in practice for predicting relative risk from  
606 *V. vulnificus* of exposure to waters of the canal and harbor.

607 The high level of predictability for system-wide average *V. vulnificus* is similar to  
608 that achieved using logistic regression to predict *vvhA* as a binary response variable  
609 either as presence vs. absence (46) or low vs. high abundance (54). Improvements  
610 in the prediction of *V. vulnificus* at higher resolution may be realized by combining  
611 biological population models for *V. vulnificus* with physical models of coastal  
612 circulation (54). In the meantime, the results from this study provide a detailed  
613 description of the ecology of *V. vulnificus* in tropical estuarine waters of Hawai'i. The  
614 results are a useful first step toward predicting and, ultimately taking steps to  
615 mitigate, the incidence of *V. vulnificus* infections.

## 616 **ACKNOWLEDGMENTS**

617 We are grateful to G. Walker and B. Marchant for assistance with sample collection  
618 and A. Culley for support and advice. We thank Hawai'i Ocean Time-series program  
619 staff for support with processing PC/PN samples and R. Briggs for advice on  
620 chemical measurements. This work was supported by grants from Hawai'i Sea Grant  
621 (2009, 2012) and the National Science Foundation (OCE05-54768, OCE08-26650)  
622 and NOAA Ocean Observing (NA07NOS4730207).

## 623 **REFERENCES**

- 624 1. Oliver J. 2006. *Vibrio vulnificus*, p. 349–363. In Thompson, F, Austin, B, Swings, J  
625 (eds.), *The Biology of Vibrios*. American Society for Microbiology (ASM),  
626 Washington, D.C.
- 627 2. Horseman MA, Surani S. 2011. A comprehensive review of *Vibrio vulnificus*: an  
628 important cause of severe sepsis and skin and soft-tissue infection. *Int J Infect*

629 Dis 15:e157–e166.

- 630 3. Jones MK, Oliver JD. 2009. *Vibrio vulnificus*: disease and pathogenesis. Infect  
631 Immun 77:1723–1733.
- 632 4. Oliver JD. 2005. Wound infections caused by *Vibrio vulnificus* and other marine  
633 bacteria. Epidemiol Infect 133:383–391.
- 634 5. Oliver JD. 2015. The biology of *Vibrio vulnificus*. Microbiol Spectr 3:VE-0001-  
635 2014.
- 636 6. Baker-Austin C, Oliver JD. 2018. *Vibrio vulnificus*: new insights into a deadly  
637 opportunistic pathogen. Environ Microbiol 20:423–430.
- 638 7. Kim MS, Jeong HD. 2001. Development of 16S rRNA targeted PCR methods for  
639 the detection and differentiation of *Vibrio vulnificus* in marine environments.  
640 Aquaculture 193:199–211.
- 641 8. Nilsson WB, Paranjype RN, DePaola A, Strom MS. 2003. Sequence  
642 polymorphism of the 16S rRNA gene of *Vibrio vulnificus* is a possible indicator  
643 of strain virulence. J Clin Microbiol 41:442–446.
- 644 9. Rosche TM, Yano Y, Oliver JD. 2005. A rapid and simple PCR analysis indicates  
645 there are two subgroups of *Vibrio vulnificus* which correlate with clinical or  
646 environmental isolation. Microbiol Immunol 49:381–389.
- 647 10. Rosche TM, Binder EA, Oliver JD. 2010. *Vibrio vulnificus* genome suggests two  
648 distinct ecotypes. Environ Microbiol Rep 2:128–132.
- 649 11. Sanjuán E, Fouz B, Oliver JD, Amaro C. 2009. Evaluation of genotypic and  
650 phenotypic methods to distinguish clinical from environmental *Vibrio vulnificus*  
651 strains. Appl Environ Microbiol 75:1604–1613.
- 652 12. Kelly MT. 1982. Effect of temperature and salinity on *Vibrio (Beneckeia)*

- 653            *vulnificus* occurrence in a Gulf Coast environment. Appl Environ Microbiol  
654            44:820–824.
- 655    13. O’Neill KR, Jones SH, Grimes DJ. 1992. Seasonal incidence of *Vibrio vulnificus* in  
656            the Great Bay estuary of New Hampshire and Maine. Appl Environ Microbiol  
657            58:3257–3262.
- 658    14. Kaysner CA, Abeyta C, Wekell MM, DePaola A, Stott RF, Leitch JM. 1987.  
659            Virulent strains of *Vibrio vulnificus* isolated from estuaries of the United States  
660            West Coast. Appl Environ Microbiol 53:1349–1351.
- 661    15. Høi L, Larsen JL, Dalsgaard I, Dalsgaard A. 1998. Occurrence of *Vibrio vulnificus*  
662            biotypes in Danish marine environments. Appl Environ Microbiol 64:7–13.
- 663    16. Motes ML, DePaola A, Cook DW, Veazey JE, Hunsucker JC, Garthright WE,  
664            Blodgett RJ, Chirtel SJ. 1998. Influence of water temperature and salinity on  
665            *Vibrio vulnificus* in Northern Gulf and Atlantic Coast oysters (*Crassostrea*  
666            *virginica*). Appl Environ Microbiol 64:1459–1465.
- 667    17. Lin M, Payne DA, Schwarz JR. 2003. Intraspecific diversity of *Vibrio vulnificus* in  
668            Galveston Bay water and oysters as determined by randomly amplified  
669            polymorphic DNA PCR. Appl Environ Microbiol 69:3170–3175.
- 670    18. Pfeffer CS, Hite MF, Oliver JD. 2003. Ecology of *Vibrio vulnificus* in estuarine  
671            waters of eastern North Carolina. Appl Environ Microbiol 69:3526–3531.
- 672    19. Randa MA, Polz MF, Lim E. 2004. Effects of temperature and salinity on *Vibrio*  
673            *vulnificus* population dynamics as assessed by quantitative PCR. Appl Environ  
674            Microbiol 70:5469–5476.
- 675    20. Rivera S, Lugo T, Hazen TC. 1989. Autecology of *Vibrio vulnificus* and *Vibrio*  
676            *parahaemolyticus* in tropical waters. Water Res 23:923–931.



- 677 21. Lipp E, Rodriguez-Palacios C, Rose J. 2001. Occurrence and distribution of the  
678 human pathogen *Vibrio vulnificus* in a subtropical Gulf of Mexico estuary.  
679 *Hydrobiologia* 460:165–173.
- 680 22. Chase E, Harwood VJ. 2011. Comparison of the effects of environmental  
681 parameters on growth rates of *Vibrio vulnificus* biotypes I, II, and III by culture  
682 and quantitative PCR analysis. *Appl Environ Microbiol* 77:4200–4207.
- 683 23. Ramirez GD, Buck GW, Smith AK, Gordon KV, Mott JB. 2009. Incidence of *Vibrio*  
684 *vulnificus* in estuarine waters of the south Texas Coastal Bend region. *J Appl*  
685 *Microbiol* 107:2047–2053.
- 686 24. Johnson CN, Flowers AR, Noriea NF, Zimmerman AM, Bowers JC, DePaola A,  
687 Grimes DJ. 2010. Relationships between environmental factors and pathogenic  
688 vibrios in the northern Gulf of Mexico. *Appl Environ Microbiol* 76:7076–7084.
- 689 25. Nigro OD, Hou A, Vithanage G, Fujioka RS, Steward GF. 2011. Temporal and  
690 spatial variability in culturable pathogenic *Vibrio* spp. in Lake Pontchartrain,  
691 Louisiana, following hurricanes Katrina and Rita. *Appl Environ Microbiol*  
692 77:5384–5393.
- 693 26. Wetz JJ, Blackwood AD, Fries JS, Williams ZF, Noble RT. 2014. Quantification of  
694 *Vibrio vulnificus* in an estuarine environment: a multi-year analysis using qPCR.  
695 *Estuaries Coasts* 37:421–435.
- 696 27. Dziuban EJ, Liang JL, Craun GF, Hill V, Yu PA, Painter J, Moore MR, Calderon RL,  
697 Roy SL, Beach MJ, Control C for D, CDC P. 2006. Surveillance for waterborne  
698 disease and outbreaks associated with recreational water—United States,  
699 2003–2004. *MMWR Surveill Summ Morb Mortal Wkly Rep Surveill Summ CDC*  
700 55:1–30.
- 701 28. Yoder JS, Hlavsa MC, Craun GF, Hill V, Roberts V, Yu PA, Hicks LA, Alexander NT,  
702 Calderon RL, Roy SL, Beach MJ, Control C for D, CDC P. 2008. Surveillance for

- 703 waterborne disease and outbreaks associated with recreational water use and  
704 other aquatic facility-associated health events—United States, 2005–2006.  
705 MMWR Surveill Summ Morb Mortal Wkly Rep Surveill Summ CDC 57:1–29.
- 706 29. Hlavsa MC, Roberts VA, Anderson AR, Hill VR, Kahler AM, Orr M, Garrison LE,  
707 Hicks LA, Newton A, Hilborn ED, Wade TJ, Beach MJ, Yoder JS, CDC. 2011.  
708 Surveillance for waterborne disease outbreaks and other health events  
709 associated with recreational water—United States, 2007–2008. MMWR Surveill  
710 Summ Morb Mortal Wkly Rep Surveill Summ CDC 60:1–32.
- 711 30. Vithanage G. 2011. The prevalence and public health significance of human  
712 pathogenic *Vibrio* species (*V. cholera*, *V. vulnificus*, *V. parahaemolyticus*, *V.*  
713 *alginolyticus*) in Hawai'i's diverse tropical coastal environments. PhD Thesis,  
714 University of Hawai'i at Mānoa, Honolulu.
- 715 31. Viau EJ, Goodwin KD, Yamahara KM, Layton BA, Sassoubre LM, Burns SL, Tong  
716 H-I, Wong SHC, Lu Y, Boehm AB. 2011. Bacterial pathogens in Hawaiian coastal  
717 streams—associations with fecal indicators, land cover, and water quality.  
718 Water Res 45:3279–3290.
- 719 32. Giambelluca TW, Chen Q, Frazier AG, Price JP, Chen YL, Chu PS, Eischeid JK,  
720 Delparte DM. 2013. Online rainfall atlas of Hawai'i. Bull Am Meteorol Soc  
721 94:313–316.
- 722 33. De Carlo EH, Anthony SS. 2002. Spatial and temporal variability of trace  
723 element concentrations in an urban subtropical watershed, Honolulu, Hawaii.  
724 Appl Geochem 17:475–492.
- 725 34. De Carlo EH, Anthony SS. 2002. Spatial and temporal variability of trace  
726 element concentrations in an urban subtropical watershed, Honolulu, Hawaii.  
727 Appl Geochem 17:475–492.
- 728 35. Laws EA, Doliente D, Hiayama J, Hokama M-L, Kim K, Li D, Minami S, Morales C.

- 729 1993. Hypereutrophication of the Ala Wai Canal, Oahu, Hawaii: prospects for  
730 cleanup. *Pac Sci* 47:59–75.
- 731 36. Gonzales F. 1971. A descriptive study of the physical oceanography of the Ala  
732 Wai Canal. PhD Thesis, University of Hawa‘i at Mānoa, Honolulu.
- 733 37. Gordon LI, Jennings Jr JC, Ross AA, Krest JM. 1994. A suggested protocol for  
734 continuous flow automated analysis of seawater nutrients (phosphate, nitrate,  
735 nitrite and silicic acid) in the WOCE Hydrographic Program and the Joint Global  
736 Ocean Flux Study. 93–1. Technical Report, Oregon State University, College of  
737 Oceanography, Descriptive Chemical Oceanography Group.
- 738 38. Tomlinson MJ, De Carlo EH, McManus MA, Pawlak G, Steward GF, Sansone FJ,  
739 Nigro OD, Timmerman RE, Patterson J, Jaramillo S, Ostrander CE. 2011.  
740 Characterizing the effects of two storms on the coastal waters of O‘ahu, Hawai‘i,  
741 using data from the Pacific Islands Ocean Observing System. *Oceanography*  
742 24:182–199.
- 743 39. Karl DM, Dore JE, Hebel DV, Winn C. 1991. Procedures for particulate carbon,  
744 nitrogen, phosphorus and total mass analyses used in the US-JGOFS Hawaii  
745 Ocean Time-series program, p. 71–77. *In* Hurd, DC, Spencer, DW (eds.), *Marine*  
746 *Particles: Analysis and Characterization*. Washington, D.C.
- 747 40. Strickland JDH, Parsons TR. 1972. A practical hand book of seawater analysis,  
748 2nd ed. Fisheries Research Board of Canada Bulletin 157.
- 749 41. Berthelet M, Whyte LG, Greer CW. 1996. Rapid, direct extraction of DNA from  
750 soils for PCR analysis using polyvinylpyrrolidone spin columns. *FEMS*  
751 *Microbiol Lett* 138:17–22.
- 752 42. Campbell MS, Wright AC. 2003. Real-time PCR analysis of *Vibrio vulnificus* from  
753 oysters. *Appl Environ Microbiol* 69:7137–7144.

- 754 43. Baker-Austin C, Gore A, Oliver JD, Rangdale R, McArthur JV, Lees DN. 2010.  
755 Rapid in situ detection of virulent *Vibrio vulnificus* strains in raw oyster  
756 matrices using real-time PCR. *Environ Microbiol Rep* 2:76–80.
- 757 44. Bustin SA, Benes V, Garson JA, Hellemans J, Huggett J, Kubista M, Mueller R,  
758 Nolan T, Pfaffl MW, Shipley GL, Vandesompele J, Wittwer CT. 2009. The MIQE  
759 Guidelines: Minimum information for publication of quantitative real-time PCR  
760 experiments. *Clin Chem* 55:611–622.
- 761 45. Deeb R, Tufford D, Scott GI, Moore JG, Dow K. 2018. Impact of climate change on  
762 *Vibrio vulnificus* abundance and exposure risk 1–15.
- 763 46. Banakar V, Constantin de Magny G, Jacobs J, Murtugudde R, Huq A, Wood RJ,  
764 Colwell RR. 2011. Temporal and spatial variability in the distribution of *Vibrio*  
765 *vulnificus* in the Chesapeake Bay: a hindcast study. *EcoHealth* 8:456–467.
- 766 47. Parvathi A, Kumar HS, Karunasagar I, Karunasagar I. 2004. Detection and  
767 enumeration of *Vibrio vulnificus* in oysters from two estuaries along the  
768 southwest coast of India, using molecular methods. *Appl Environ Microbiol*  
769 70:6909–6913.
- 770 48. De Carlo EH, Hoover DJ, Young CW, Hoover RS, Mackenzie FT. 2007. Impact of  
771 storm runoff from tropical watersheds on coastal water quality and  
772 productivity. *Appl Geochem* 22:1777–1797.
- 773 49. Goldberg S, Sposito G. 1984. Chemical model of phosphate adsorption by soils:  
774 I. Reference oxide minerals. *Soil Sci Soc Am J* 48:772–778.
- 775 50. Creamer B. 2006. Bacteria draw attention of UH scientists. *Honol Advert*.  
776 Honolulu.
- 777 51. Williams TC, Froelich BA, Phippen B, Fowler P, Noble RT, Oliver JD. 2017.  
778 Different abundance and correlational patterns exist between total and

- 779 presumed pathogenic *Vibrio vulnificus* and *V. parahaemolyticus* in shellfish and  
780 waters along the North Carolina coast. FEMS Microbiol Ecol 93:125–11.
- 781 52. Lin M, Schwarz JR. 2003. Seasonal shifts in population structure of *Vibrio*  
782 *vulnificus* in an estuarine environment as revealed by partial 16S ribosomal  
783 DNA sequencing. FEMS Microbiol Ecol 45:23–27.
- 784 53. Maugeri TL, Carbone M, Fera MT, Gugliandolo C. 2006. Detection and  
785 differentiation of *Vibrio vulnificus* in seawater and plankton of a coastal zone of  
786 the Mediterranean Sea. Res Microbiol 157:194–200.
- 787 54. Jacobs JM, Rhodes M, Brown CW, Hood RR, Leight A, Long W, Wood R. 2014.  
788 Modeling and forecasting the distribution of *Vibrio vulnificus* in Chesapeake  
789 Bay. J Appl Microbiol 117:1312–1327.
- 790

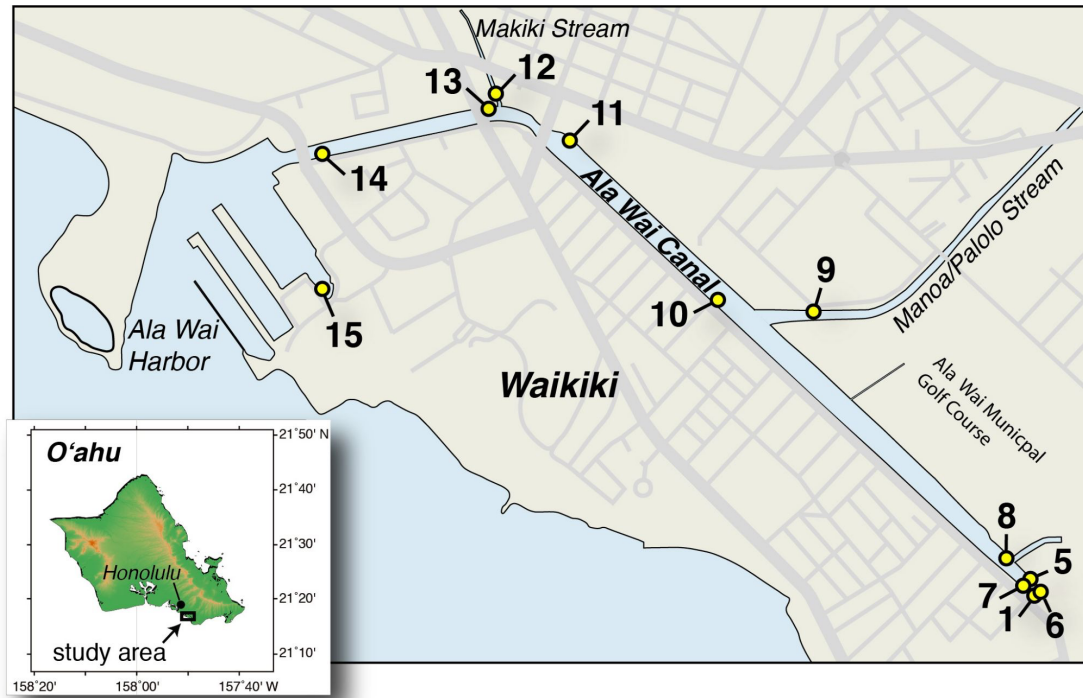
791 **Table 1.** Variables measured on individual samples, the number of samples measured, and the  
792 geometric mean (geomean), mean, median, minimum (min) and maximum (max) values for each  
793 (reported to two significant digits).

<b>Variable</b>	<b>units</b>	<b>n</b>	<b>Geomean</b>	<b>Mean</b>	<b>Median</b>	<b>S.D.</b>	<b>Min</b>	<b>Max</b>
Temperature	°C	242	27	27	27	2.6	19	32
Salinity	ppt	243	20	24	28	9.7	1	36
Nitrate	µM	209	18	37	17	48	0.02	260
Nitrite	µM	211	0.47	0.59	0.47	0.47	0.04	3.3
Ammonia	µM	207	5.5	6.7	5.7	4.3	0.94	22
Phosphate	µM	211	1	1.3	0.95	1.1	0.2	8.7
Silica	µM	211	110	140	120	92	11	490
Particulate Carbon	µM	199	130	250	120	650	20	7500
Particulate Nitrogen	µM	199	16	26	14	51	2.6	560
Chlorophyll <i>a</i>	µg L <sup>-1</sup>	194	7.6	19	7.3	43	0.4	500
Total bacteria	10 <sup>9</sup> cells L <sup>-1</sup>	219	4.2	4.8	4.7	2.3	0.47	11
CaV blue <sup>1</sup>	CFU mL <sup>-1</sup>	59	130	400	100	770	12	3904
<i>vvhA</i> gene <sup>2</sup>	copies mL <sup>-1</sup>	239	68	330	60	1200	3.4	14000

794  
795  
796

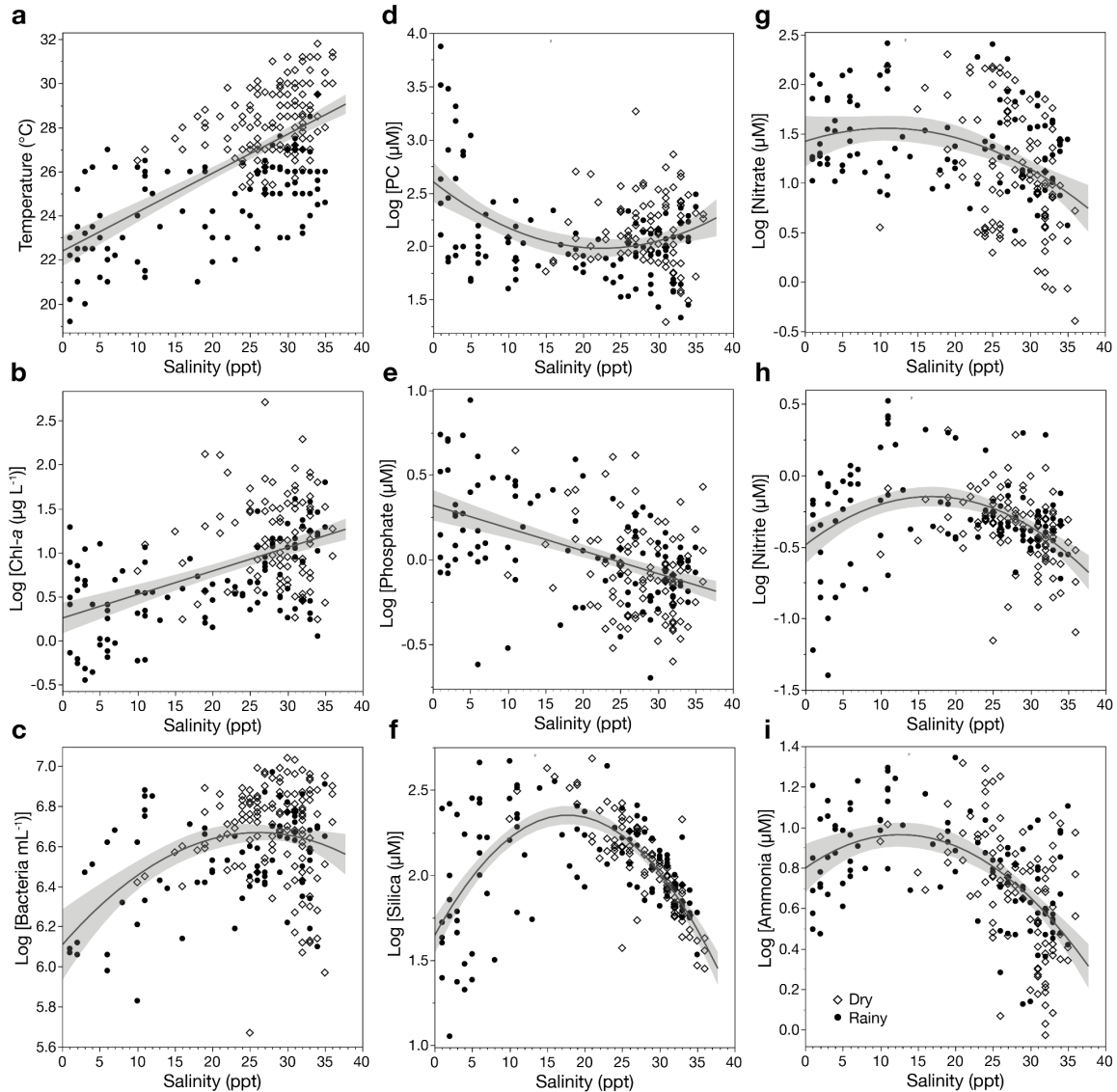
<sup>1</sup> culture-based blue colony forming units (CFU) when plating on CHROMagar Vibrio medium (CaV)

<sup>2</sup> qPCR-based estimates



797

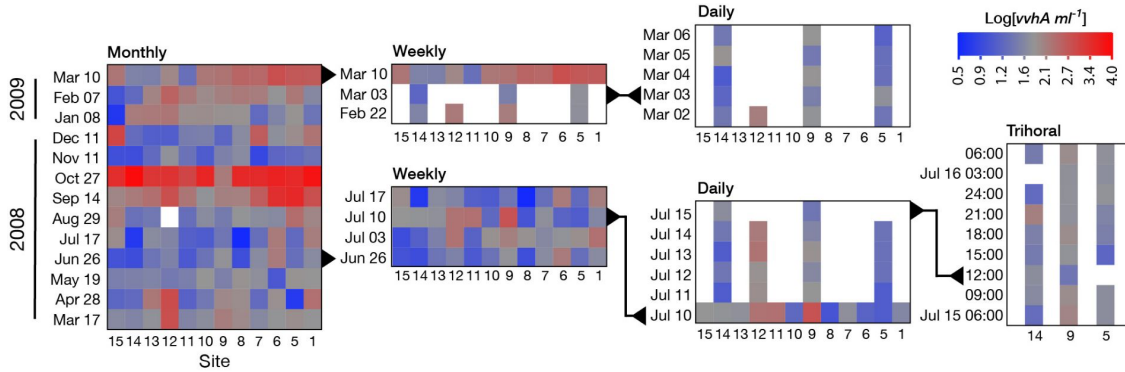
798 **Fig. 1.** Map of Sampling Sites. Inset shows the general location of the canal on the  
799 south shore of the island of O‘ahu in the Hawaiian Island chain. Main map shows the  
800 site numbers and position along the canal. Site 1 is at the closed end of the canal  
801 with occasional input from surface runoff via storm drains. Sites 9 and 12 are at the  
802 mouths of the Mānoa-Palolo and Makiki Streams, respectively.



803

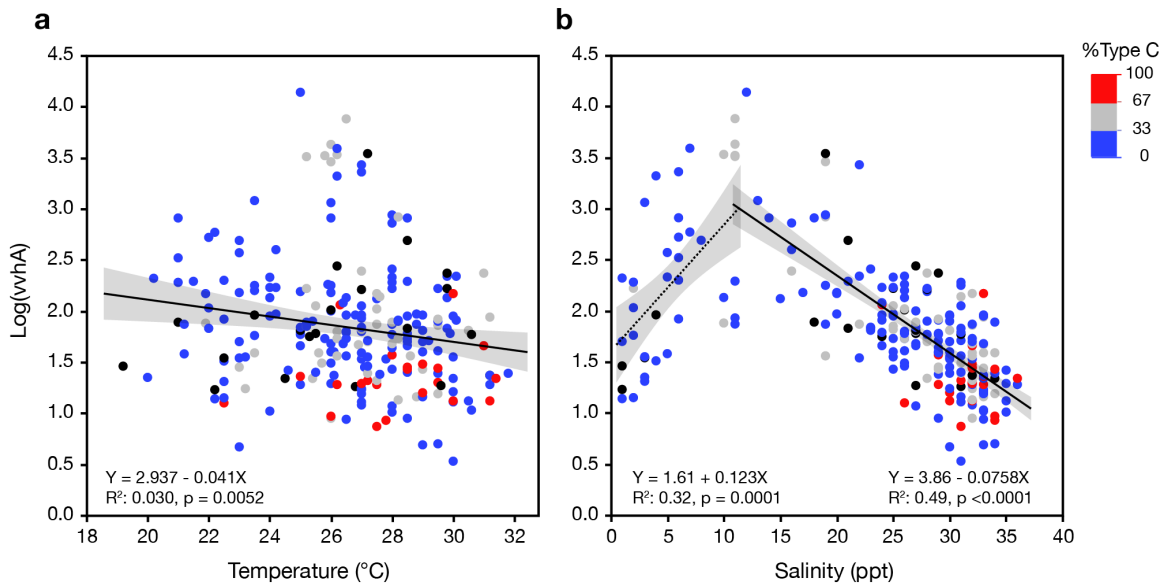
804 **Fig. 2.** Variability in measured biological and chemical properties of samples as a  
805 function of salinity in samples from the rainy (solid circles) and dry (open  
806 diamonds) seasons. Regressions against salinity are shown for (a) temperature ( $r^2 =$   
807 0.42), (b) Log chl *a* ( $r^2 = 0.24$ ), (c) log bacteria ( $r^2 = 0.14$ ), (d) log PC ( $r^2 = 0.13$ ), (e)  
808 log phosphate ( $r^2 = 0.22$ ), (f) log silica ( $r^2 = 0.463$ ), (g) log nitrate ( $r^2 = 0.13$ ), (h) log  
809 nitrite ( $r^2 = 0.152$ ), (i) log ammonia ( $r^2 = 0.29$ ). Regression lines and 95%  
810 confidence limits were fit using only first order terms unless addition of a quadratic  
811 term substantially improved  $r^2$  or reduced root mean square error. All fits were  
812 significant ( $p < .0001$ ).





813

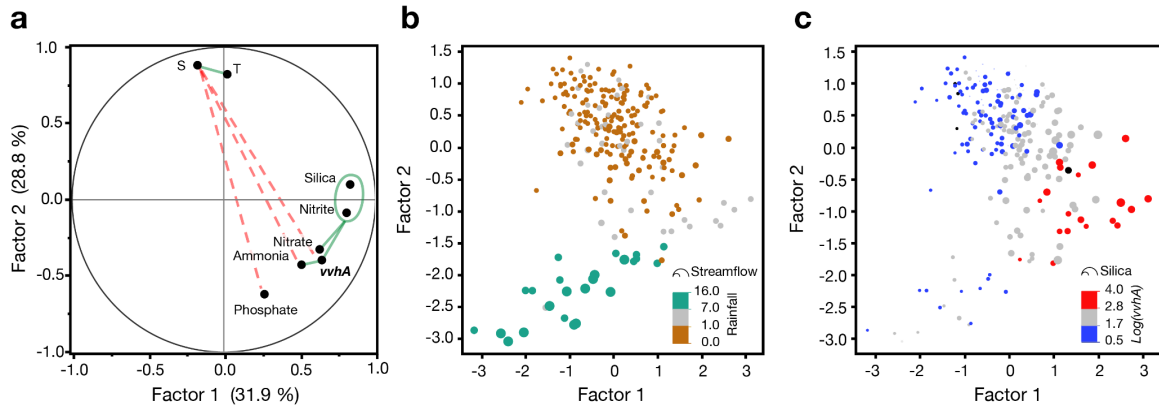
814 **Fig. 3.** Heat maps illustrating spatial and temporal variability in *V. vulnificus*.  $\text{Log } vvha$   
 815 concentrations are color coded at each station over time for monthly, weekly, daily and  
 816 trihoral sampling events. The overall average  $\text{log}(vvha)$  from all samplings of 1.8 is shown in  
 817 grey. Concentrations above average are in red and those below average in blue. The  
 818 samplings on different time scales are nested and the events that are overlapping in the  
 819 different graphs are indicated with black triangles and lines.



820

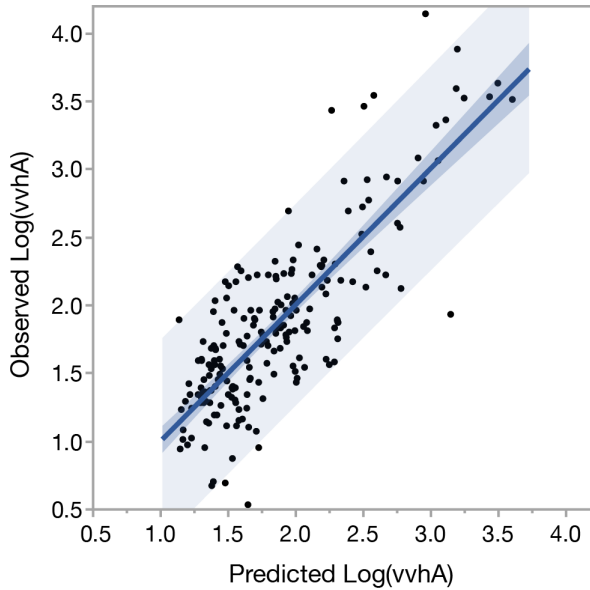
821 **Fig. 4.** Concentration of *vvha* as a function of **a)** temperature or **b)** salinity. The percentage  
 822 of total *vvha* that derives from “C-type” *V. vulnificus* was determined as the ratio of *vcgC* (C-  
 823 type) and *vvha* (total *V. vulnificus*) gene concentrations and is indicated by the color scale.  
 824 Blue dots are samples dominated by E-type, red dots by C-type.

825



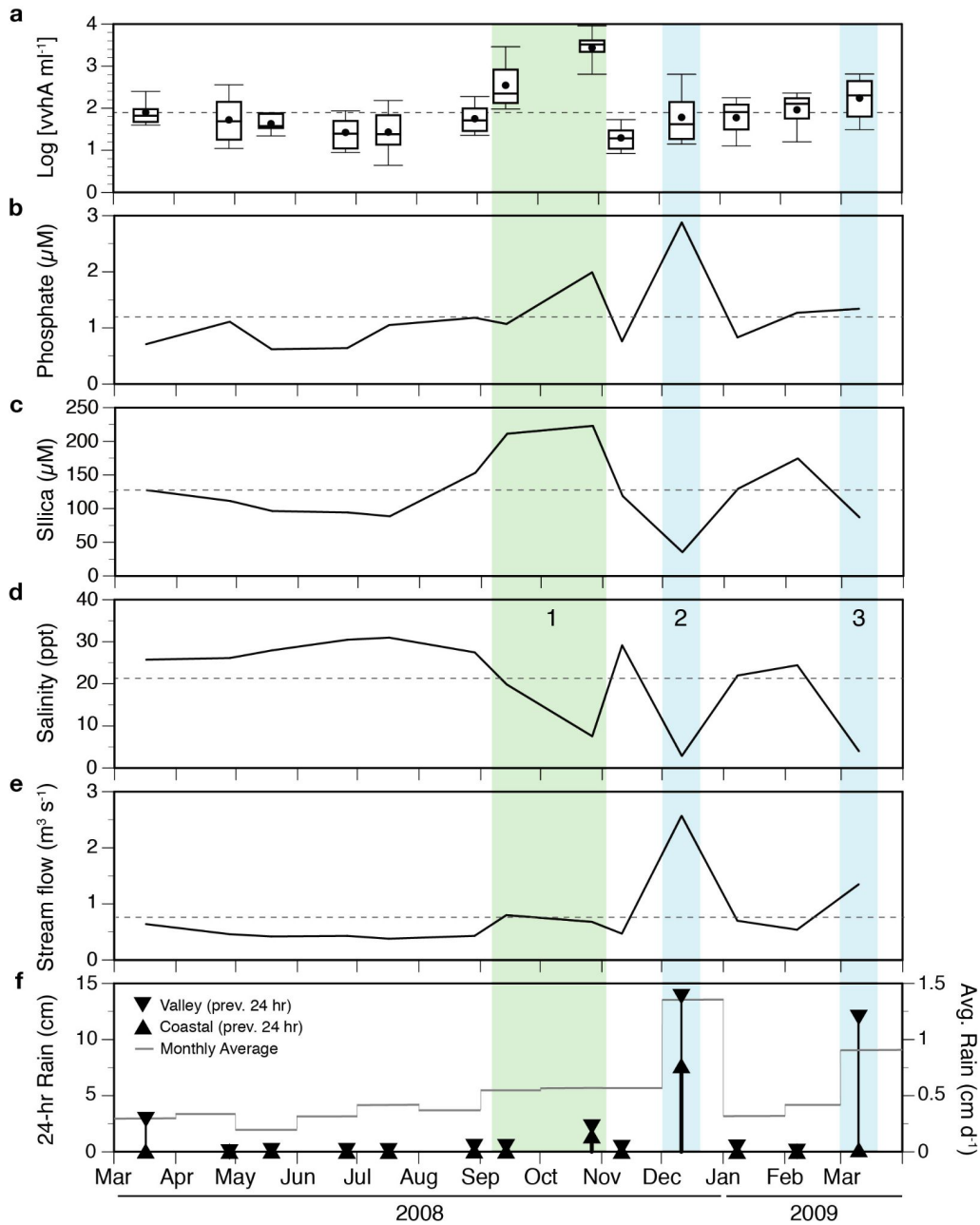
826

827 **Fig. 5.** Factor Analysis for *vvhA*, temperature, salinity, and nutrients. **(a)** The factor loading  
828 plot for factors 1 and 2 (eigenvalues >1). Variables with a strong positive correlations ( $r \geq$   
829 0.4) are connected by green solid lines and those with strong negative correlation ( $r \leq 0.4$ )  
830 are connected by dashed red lines **(b)** Plot of the factor scores for the data with points  
831 colored by 24-hr antecedent rainfall in Mānoa Valley (in cm) and scaled in size so area is  
832 proportional to streamflow in the Mānoa-Palolo Stream. **(c)** Plot of the factor scores with  
833 data points colored according to  $\log vvhA$  concentration and scaled in size so area is  
834 proportional to silica concentration.



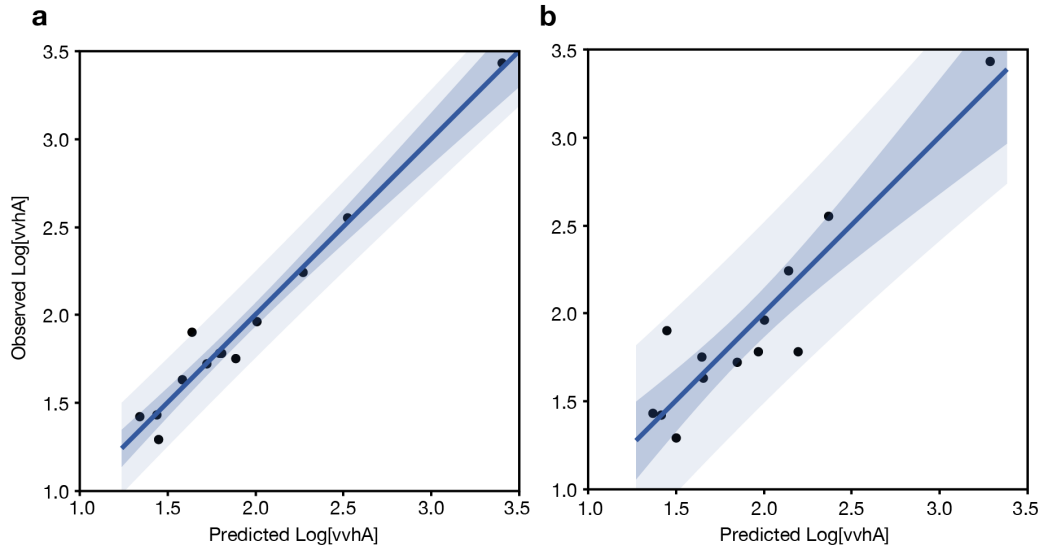
835

836 **Fig. 6.** Observed vs. predicted values of log transformed *vvhA* gene copies per mL<sup>-1</sup>.  
837 Predicted values are combined from two separate models (one for samples < 12 ppt, one for  
838 ≥ 12 ppt). Predicted values are restricted to individual samples for which all of the  
839 predictor variables were measured within a given salinity range (n = 204 out of 239 in  
840 total). Darker and lighter shading illustrates the 95% confidence limits of the fit and  
841 prediction, respectively. Combined, the models explain a significant amount of the variation  
842 in the observations:  $r^2 = 0.661$ , RMSE = 0.37, F Test (1, 204) = 396.90,  $p < .0001$ .



843

844 **Fig. 7.** Time series of variables in or influencing the Ala Wai Canal system. Shown are **a)**  
845 variations of *vvhA* concentrations as box plots of all log transformed values measured at  
846 every site at each monthly sampling, canal-wide geometric means of **b)** phosphate, **c)**  
847 salinity, **d)** silica, as well as **e)** streamflow in the Mānoa-Palolo stream on the day of  
848 sampling, and **f)** rainfall in the 24-hr period preceding sampling as measured at the  
849 Honolulu coastal (upward triangles) and Mānoa Valley rain gauges (downward triangles).  
850 Daily rainfall average for the month is shown as the mean for both sites (grey line).



851

852 **Fig. 8.** Observed vs predicted canal-wide average of log-transformed *vwhA* concentrations.  
853 Predictions are derived from **a**) the best subset of variables (salinity, silica, streamflow,  
854 particulate carbon) from generalized regression model ( $r^2 = 0.97$ ; RMSE = 0.11; F test  $p <$   
855 .0001) or **b**) a restricted subset of two variables (rainfall and salinity) that are easily  
856 measured autonomously ( $r^2 = 0.86$ ; RMSE = 0.22; F test  $p <$ .0001). Darker and lighter  
857 shading illustrates the 95% confidence limits of the fit and prediction, respectively.